

# Supporting Information

## **Self-assembly of two supramolecular indium(III) metal-organic frameworks for reversible iodine capture and large band gap change semiconductor behavior**

Xi Du,<sup>a</sup> Ruiqing Fan,<sup>\*,a</sup> Jizhuang Fan,<sup>\*,b</sup> Liangsheng Qiang,<sup>a</sup> Yang Song,<sup>a</sup> Yuwei Dong,<sup>a</sup> Kai Xing,<sup>a</sup> Ping Wang,<sup>a</sup> and Yulin Yang<sup>\*,a</sup>

<sup>a</sup> *MIIT Key Laboratory of Critical Materials Technology for New Energy Conversion and Storage, School of Chemistry and Chemical Engineering, Harbin Institute of Technology, Harbin 150001, P. R. of China*

<sup>b</sup> *State Key Laboratory of Robotics and System, Harbin Institute of Technology, Harbin 150001, P. R. of China*

## Index

	Content	Page No.
<b>Table S1</b>	Selected bond lengths and bond angles for <b>1</b> and <b>2</b>	<b>3</b>
<b>Table S2</b>	Selected bond lengths and bond angles for <b>1</b> and <b>2</b>	<b>4</b>
<b>Fig. S1</b>	Structural information for <b>1</b>	<b>5</b>
<b>Fig. S2</b>	Structural information for <b>1</b>	<b>5</b>
<b>Fig. S3</b>	Structural information for <b>2</b>	<b>6</b>
<b>Fig. S4</b>	Structural information for <b>2</b>	<b>6</b>
<b>Fig. S5</b>	<sup>1</sup> H NMR spectra of <b>2-QLBM</b> , <b>1</b> and <b>2</b>	<b>7</b>
<b>Fig. S6</b>	Infrared spectra of <b>2-QLBM</b> , <b>1</b> , <b>2</b> and <b>I<sub>2</sub>@2a</b>	<b>8</b>
<b>Table S3</b>	Elemental analysis results of <b>1a</b> , <b>2a</b> and <b>I<sub>2</sub>@2a</b>	<b>9</b>
<b>Fig. S7</b>	Thermal gravimetric curves of <b>1</b> and <b>1a</b>	<b>9</b>
<b>Fig. S8</b>	Nitrogen adsorption isotherms of <b>1a</b> and <b>2a</b> at 77 K	<b>9</b>
<b>Fig. S9</b>	Luminescence intensity of <b>I<sub>2</sub>@2a</b> after immersed in ethanol for 0~75 min	<b>10</b>
<b>Fig. S10</b>	Desorption efficiency of <b>I<sub>2</sub>@2a</b> in serial recycle tests.	<b>10</b>
<b>Fig. S11</b>	PXRD patterns of <b>1</b> and <b>1a</b>	<b>11</b>
<b>Fig. S12</b>	PXRD patterns of <b>2</b> , <b>2a</b> , <b>2a</b> after adsorbing I <sub>2</sub> in the first cycle and <b>2a</b> after releasing I <sub>2</sub> in the first cycle	<b>11</b>
<b>Fig. S13</b>	Emission spectra of ligands in the solid state at 298 K	<b>12</b>
<b>Fig. S14</b>	Luminescence decay curves of <b>1</b> and <b>2</b> in the solid state at 298 and 77 K	<b>12</b>
<b>Table S4</b>	Luminescent data for <b>1</b> and <b>2</b>	<b>12</b>
<b>Fig. S15</b>	Nyquist plots of the pellet sample compound <b>1</b> and <b>2</b> at 25 °C and 98% RH.	<b>13</b>

**Table S1** Selected bond lengths (Å) and bond angles (°) for **1** and **2**

<b>1</b>			
In(1)-O(4)	2.263(4)	In(1)-Cl(1)	2.457(1)
In(1)-O(2)	2.266(4)	In(1)-Cl(3)	2.476(1)
In(1)-O(3)	2.435(4)	In(1)-Cl(2)	2.475(1)
In(1)-O(1)	2.438(4)	O(4)-In(1)-Cl(2)	90.01(16)
O(4)-In(1)-O(2)	175.58(13)	O(2)-In(1)-Cl(2)	90.67(16)
O(4)-In(1)-O(3)	55.61(12)	O(3)-In(1)-Cl(2)	82.51(12)
O(2)-In(1)-O(3)	128.81(13)	O(1)-In(1)-Cl(2)	89.56(12)
O(4)-In(1)-O(1)	129.09(13)	Cl(1)-In(1)-Cl(2)	94.89(9)
O(2)-In(1)-O(1)	55.29(12)	O(4)-In(1)-Cl(3)	90.38(16)
O(3)-In(1)-O(1)	73.90(11)	O(2)-In(1)-Cl(3)	89.72(16)
O(4)-In(1)-Cl(1)	87.67(10)	O(3)-In(1)-Cl(3)	89.45(12)
O(2)-In(1)-Cl(1)	87.92(9)	O(1)-In(1)-Cl(3)	82.42(12)
O(3)-In(1)-Cl(1)	143.07(9)	Cl(1)-In(1)-Cl(3)	95.15(9)
O(1)-In(1)-Cl(1)	143.03(9)	Cl(2)-In(1)-Cl(3)	169.96(5)
<b>2</b>			
In(1)-O(1)	2.157(6)	O(1)-In(1)-N(1)	74.6(2)
In(1)-N(2)	2.206(6)	N(2)-In(1)-N(1)	71.3(2)
In(1)-N(4)	2.314(6)	N(4)-In(1)-N(1)	100.3(2)
In(1)-Cl(2)	2.406(2)	Cl(2)-In(1)-N(1)	85.20(16)
In(1)-Cl(1)	2.418(2)	Cl(1)-In(1)-N(1)	166.97(17)
In(1)-N(1)	2.461(6)	O(3)-In(2)-N(5)	85.4(2)
In(2)-O(3)	2.183(6)	O(3)-In(2)-N(8)	73.3(2)
In(2)-N(5)	2.203(6)	N(5)-In(2)-N(8)	158.1(2)
In(2)-N(8)	2.301(6)	O(3)-In(2)-Cl(4)	100.69(16)
In(2)-Cl(4)	2.412(2)	N(5)-In(2)-Cl(4)	96.95(18)
In(2)-Cl(3)	2.418(2)	N(8)-In(2)-Cl(4)	91.84(17)
In(2)-N(7)	2.427(6)	O(3)-In(2)-Cl(3)	157.20(16)
O(1)-In(1)-N(2)	86.1(2)	N(5)-In(2)-Cl(3)	97.89(18)
O(1)-In(1)-N(4)	73.4(2)	N(8)-In(2)-Cl(3)	100.01(19)
N(2)-In(1)-N(4)	159.4(2)	Cl(4)-In(2)-Cl(3)	101.29(8)
O(1)-In(1)-Cl(2)	156.03(16)	O(3)-In(2)-N(7)	74.8(2)
N(2)-In(1)-Cl(2)	99.69(17)	N(5)-In(2)-N(7)	72.9(2)
N(4)-In(1)-Cl(2)	98.23(17)	N(8)-In(2)-N(7)	96.3(2)
O(1)-In(1)-Cl(1)	99.96(16)	Cl(4)-In(2)-N(7)	169.00(16)
N(2)-In(1)-Cl(1)	96.79(18)	Cl(3)-In(2)-N(7)	84.56(16)
N(4)-In(1)-Cl(1)	89.22(17)	Cl(2)-In(1)-Cl(1)	102.39(9)

**Table S2** Important hydrogen bond and  $\pi\cdots\pi$  stacking interactions for **1** and **2**

	Coordination number	D–H $\cdots$ A	D–H/Å	H $\cdots$ A/Å	D $\cdots$ A/Å	D–H $\cdots$ A/ $^\circ$	structure
<b>1</b>	7	C8–H8A $\cdots$ O2	0.930	2.718	3.564	151.676(1)	3D
		C18–H18A $\cdots$ O4	0.929	2.731	3.591	151.133(1)	
<b>2</b>	6	C35–H35A $\cdots$ O3	0.950	2.230	3.199	157.153(3)	3D
		C8–H8A $\cdots$ O1	0.950	2.504	3.411	159.580(2)	
		C16–H16A $\cdots$ O2	0.950	2.554	3.216	126.921(1)	
		C49–H49A $\cdots$ C11	0.951	2.692	3.611	162.739(1)	
		C41–H41A $\cdots$ C13	0.949	2.820	3.629	143.757(2)	
		$\pi_{C_{g1}}-\pi_{C_{g1}}$				3.629	
$\pi_{C_{g2}}-\pi_{C_{g2}}$				3.672			

$C_{gI}$  = benzene ring

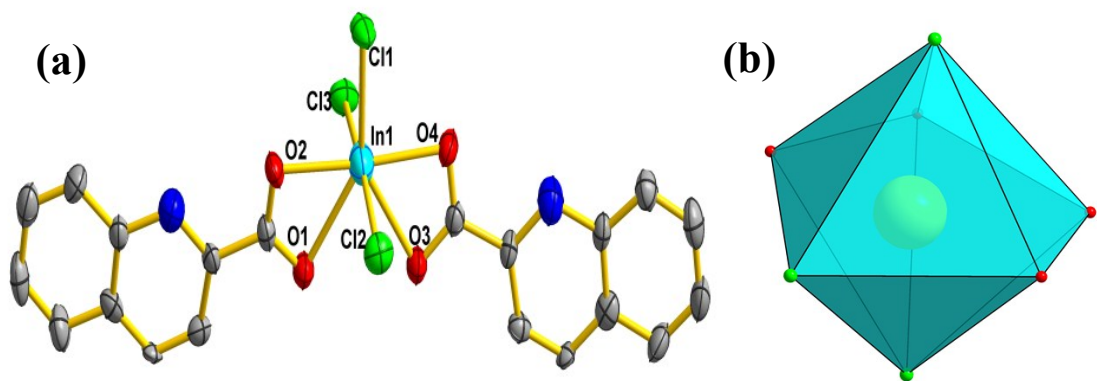


**Fig. S1** (a) X-ray structure of compound **1**, H atoms for clarity. Thermal ellipsoid is drawn at 50% probability. (b) Polyhedral of the In(III) centre in **1**.

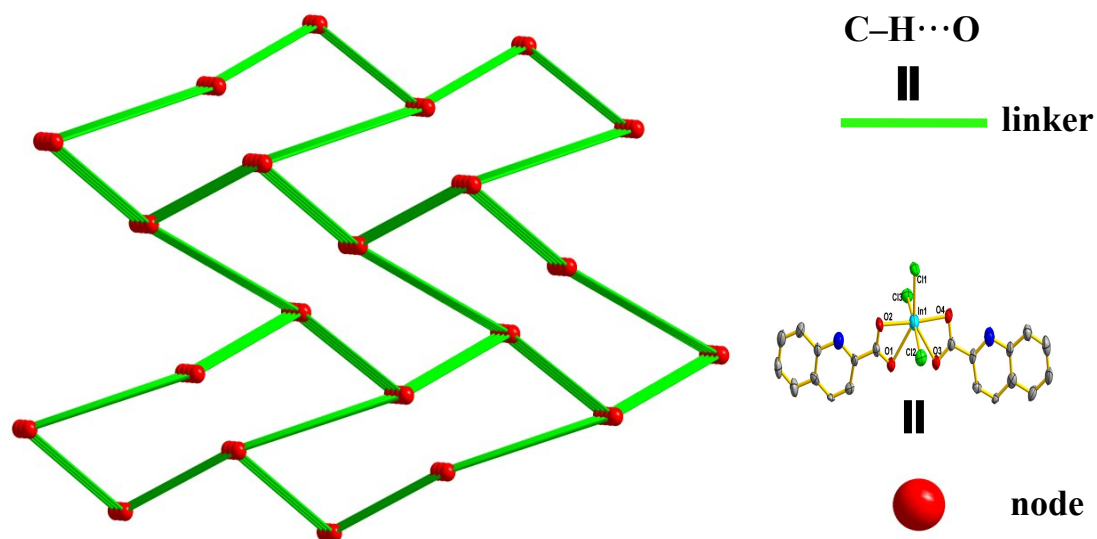


**Fig. S2** Topological view of the three-dimensional structure of compound **1**.

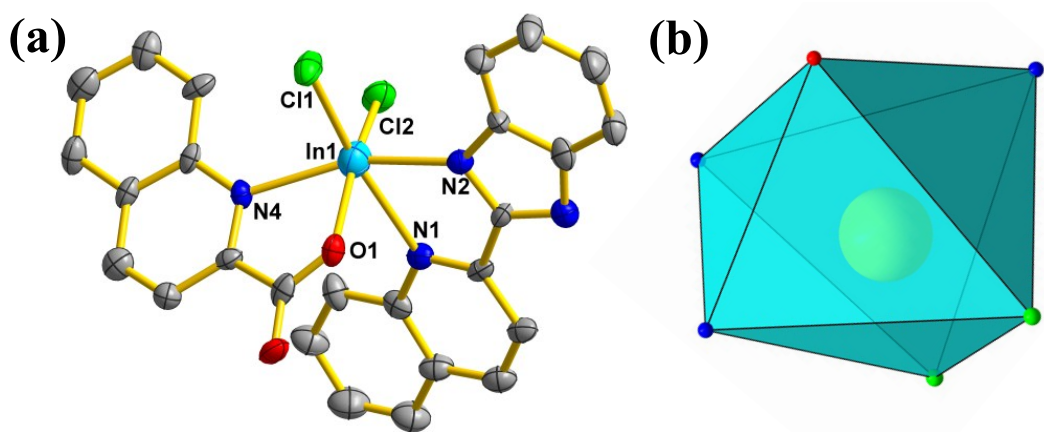


**Fig. S3** (a) X-ray structure of compound **2**, H atoms for clarity. Thermal ellipsoid is drawn at 50% probability. (b) Polyhedral of the In(III) centre in **2**.

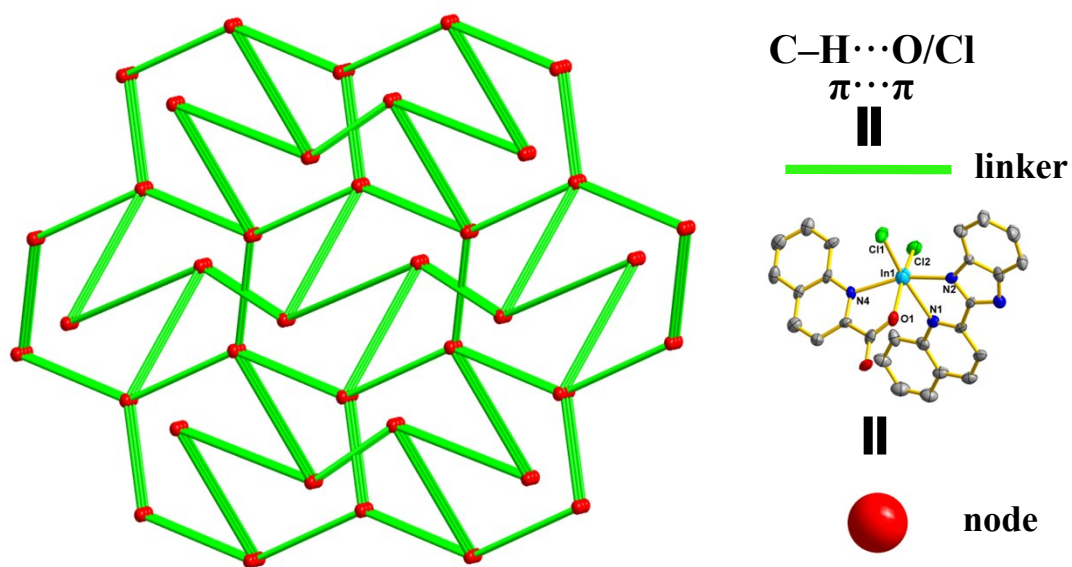


**Fig. S4** Topological view of the three-dimensional structure of compound **2**.

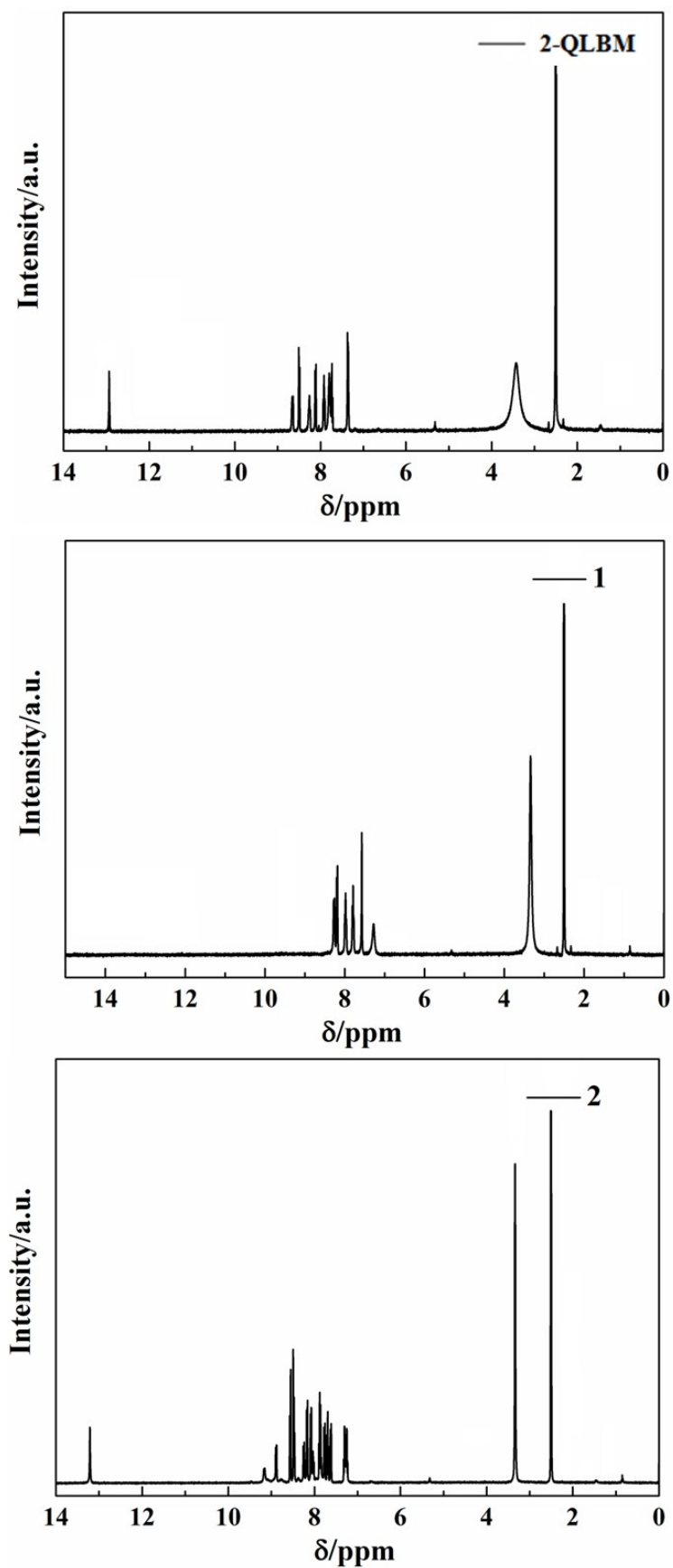


**Fig. S5**  $^1\text{H}$  NMR spectra of 2-QLBM, 1 and 2.

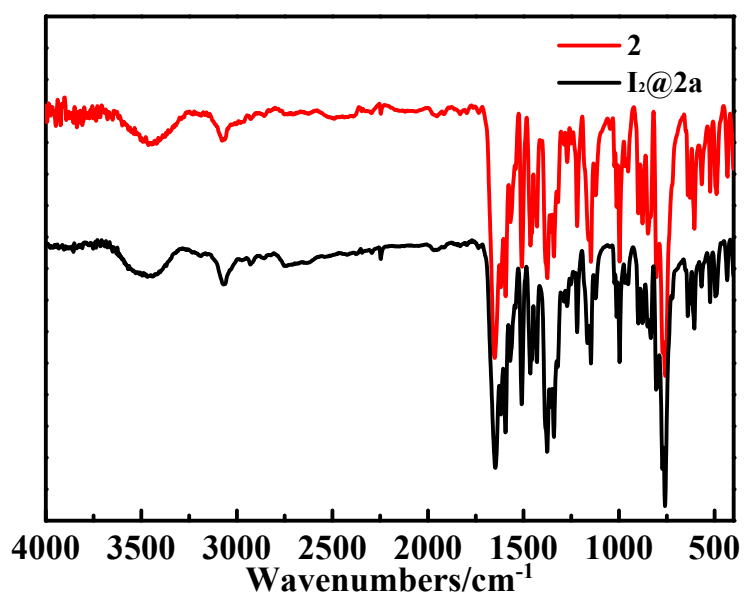
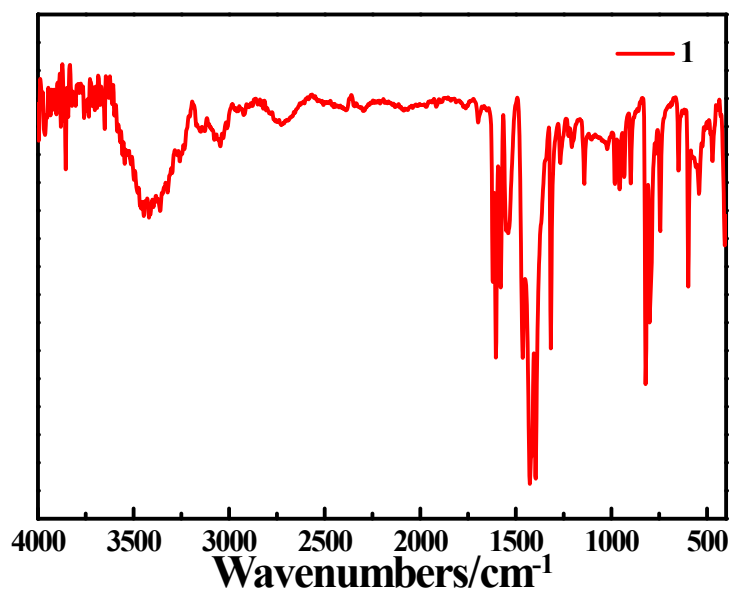
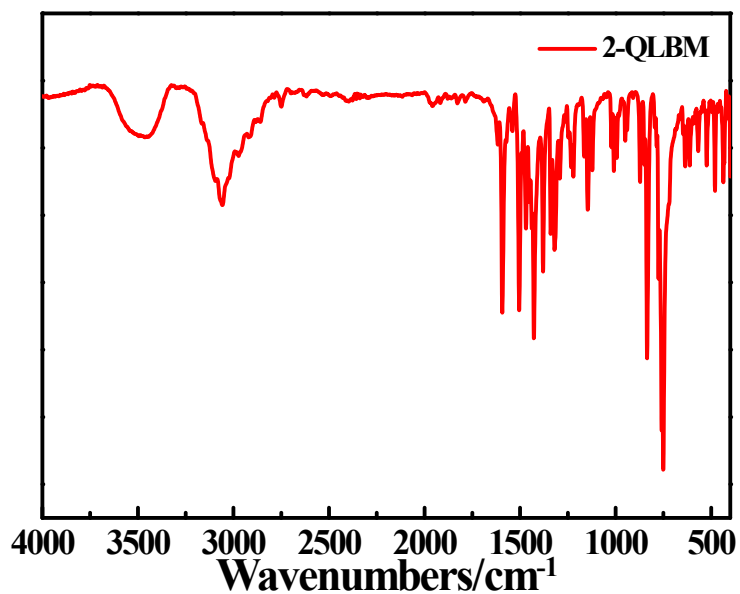


Fig. S6 IR spectra of 2-QLBM, 1, 2 and I<sub>2</sub>@2.



**Table S3** Elemental analysis results of activated compounds<sup>a</sup> and after iodine uptake in solvent<sup>a</sup>

Compound	C%	H%	N%
<b>1a</b>	42.35 (42.33)	2.48 (2.49)	4.91 (4.94)
<b>2a</b>	51.13 (51.10)	2.81 (2.80)	9.15 (9.17)
<b>I<sub>2</sub>@2a</b>	40.69 (40.66)	2.57 (2.56)	7.91 (7.93)

<sup>a</sup>Theoretical results are given in parentheses

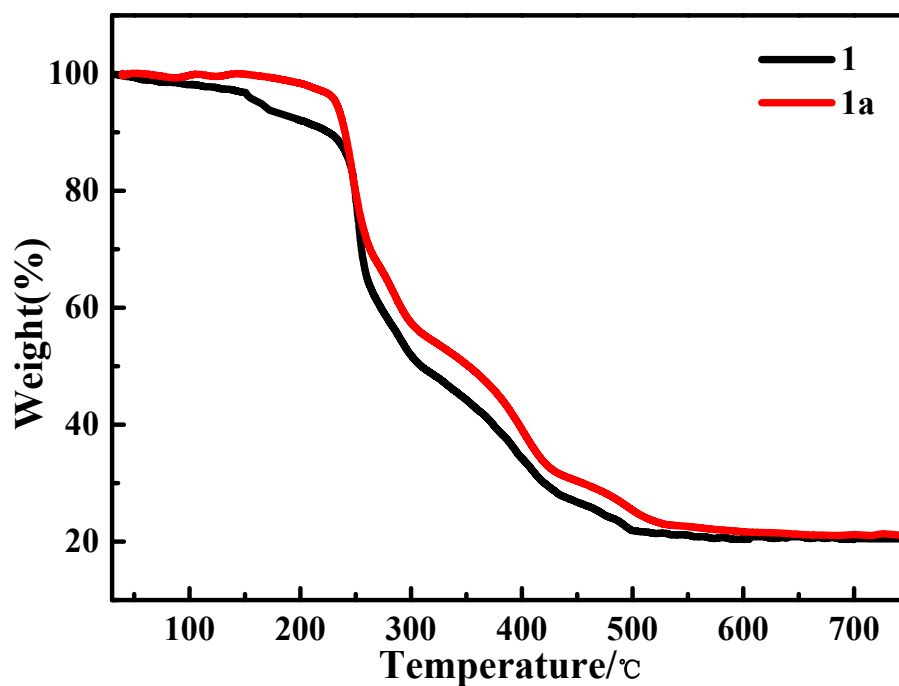


**Fig. S7** Thermal gravimetric curves for **1** and **1a**.

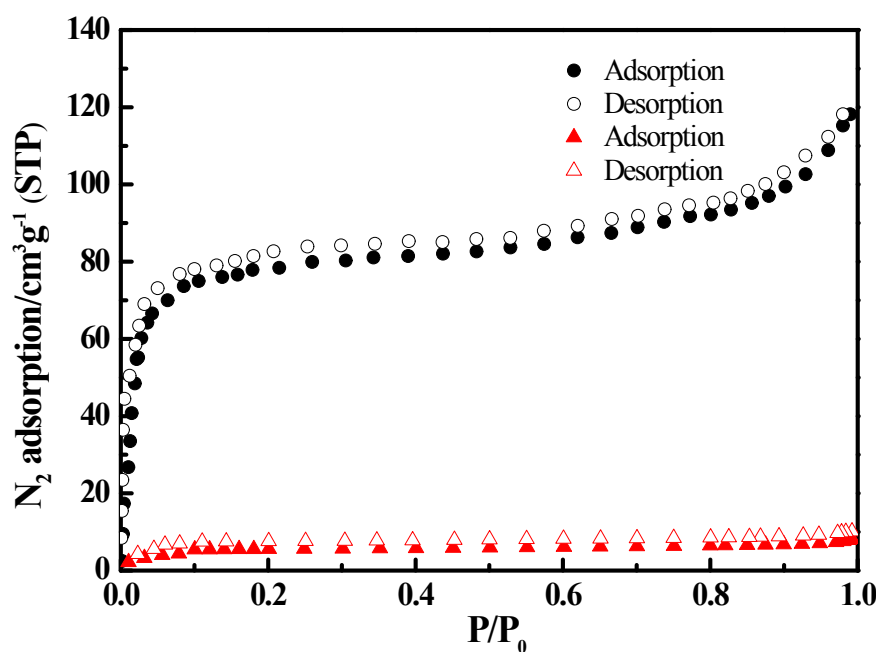


**Fig. S8** Nitrogen adsorption isotherms of **1a** (red) and **2a** (black) at 77 K.

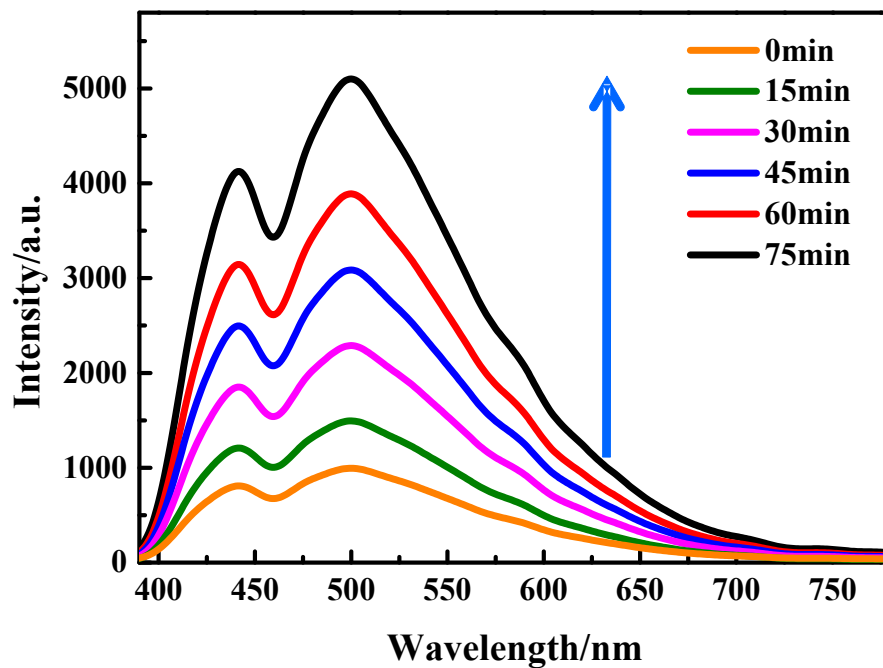


**Fig. S9** After immersed in ethanol for 0~75 min, the luminescence intensity of  $I_2@2a$  was gradually recovered.

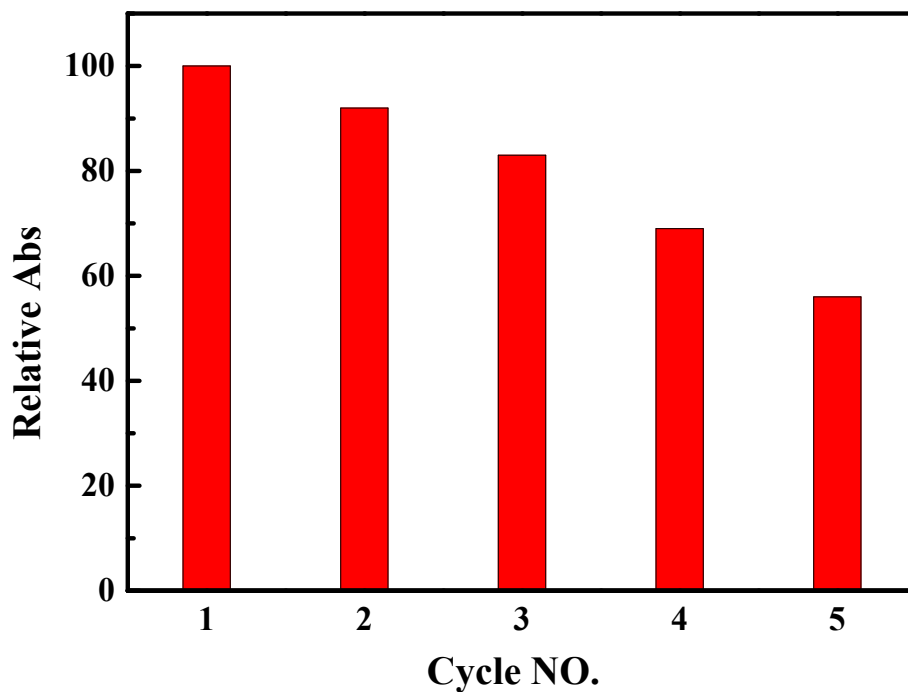


**Fig. S10** Desorption efficiency of  $I_2@2a$  in serial recycle tests.

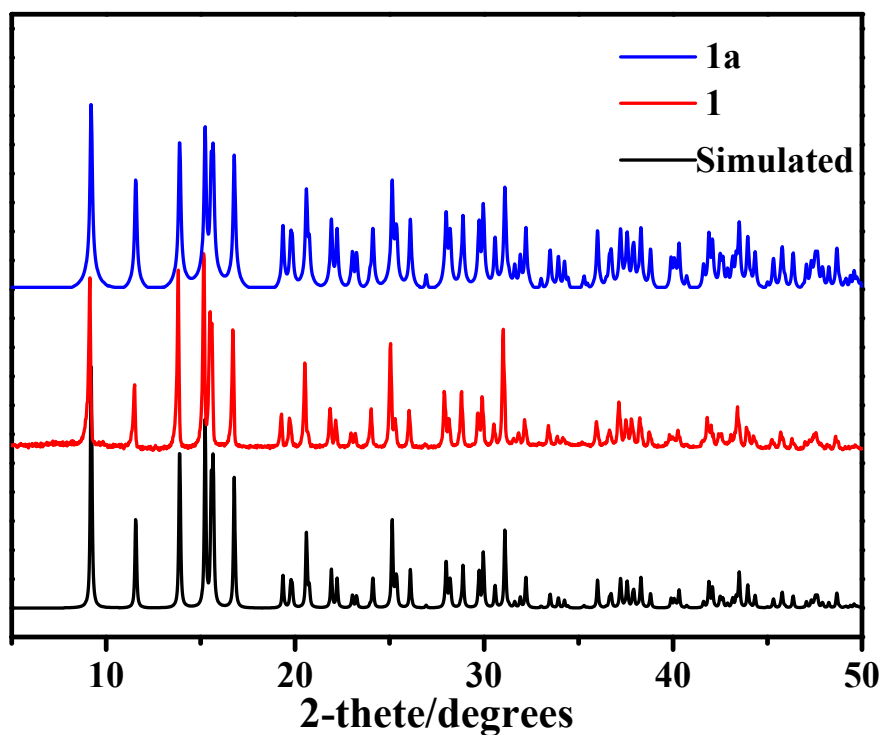


Fig. S11 PXR D patterns of 1 and 1a with the relevant simulated pattern.

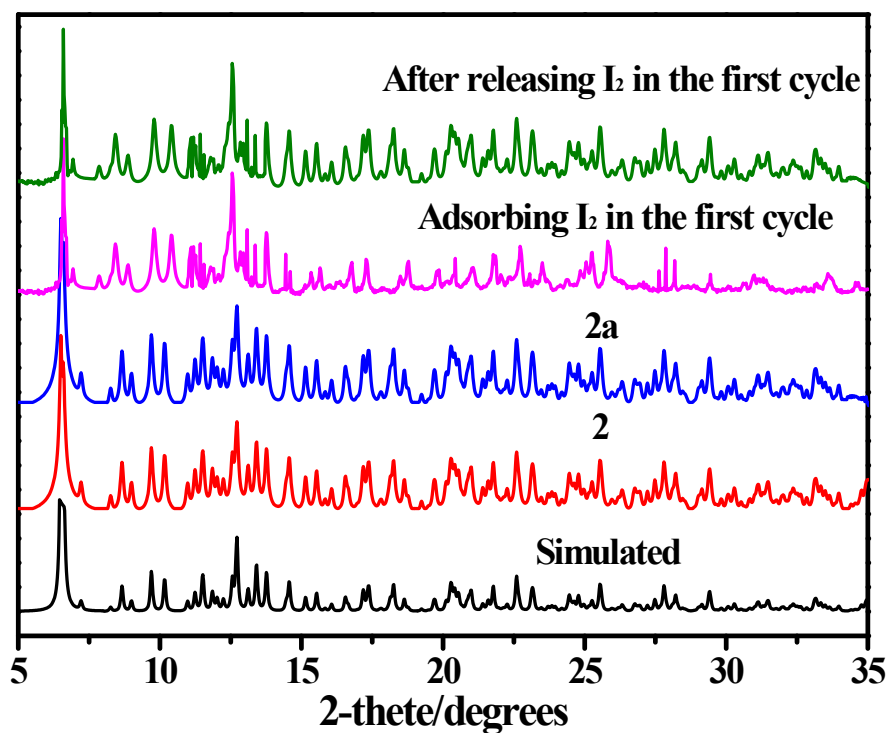
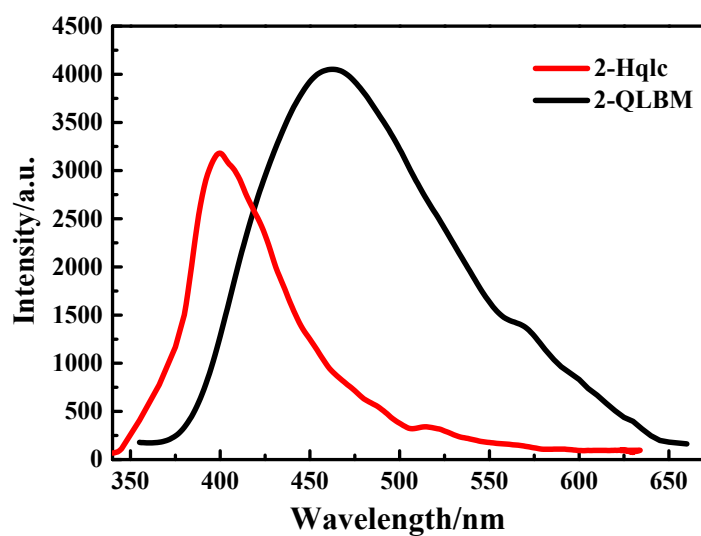
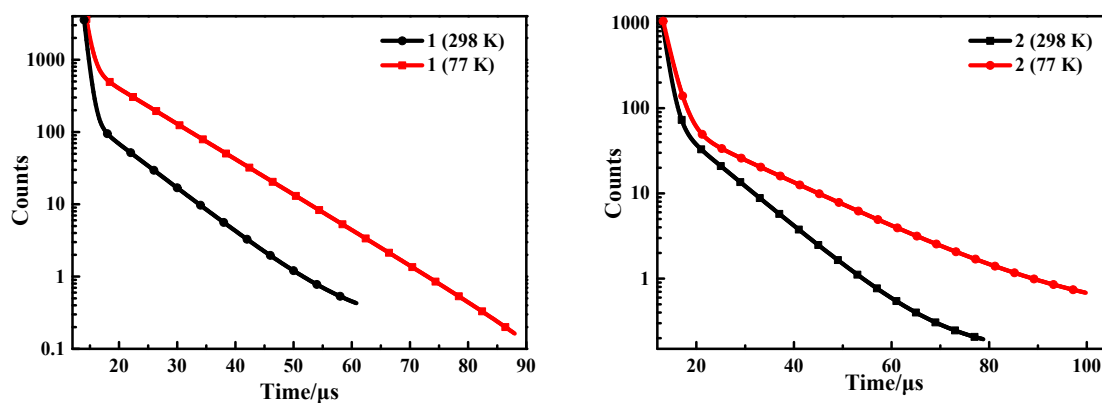


Fig. S12 PXR D patterns of 2, 2a, 2a after adsorbing I<sub>2</sub> in the first cycle and 2a after releasing I<sub>2</sub> in the first cycle with the relevant simulated pattern.



**Fig. S13** Emission spectra of free 2-Hqlc and 2-QLBM ligands in the solid state at 298 K.



**Fig. S14** Luminescence decay curves of **1** and **2** in the solid state at 298 and 77K.

**Table S4** Luminescent data for **1** and **2**

Compound	Excitation ( $\lambda$ , nm)	Emission ( $\lambda_{\text{max}}$ , nm)	CIE (x, y)	Lifetime ( $\mu\text{s}$ )		$\langle\tau\rangle$ ( $\mu\text{s}$ )	Conditions <sup>a</sup>
				$\tau_1$	$\tau_2$		
<b>1</b>	390	426	0.18, 0.08	0.60	7.09	5.98	Solid, 298 K
	390	475	0.25, 0.33	0.75	8.89	8.61	Solid, 77 K
<b>2</b>	390	443 <sup>sh</sup> , 498	0.16, 0.18	1.07	9.16	7.81	Solid, 298 K
	390	529 <sup>sh</sup> , 605	0.43, 0.50	1.64	16.32	14.26	Solid, 77 K

<sup>a</sup>Concentration in DMSO, CH<sub>3</sub>CN, CH<sub>3</sub>OH and CHCl<sub>3</sub> solution:  $c = 1 \times 10^{-6}$  M.

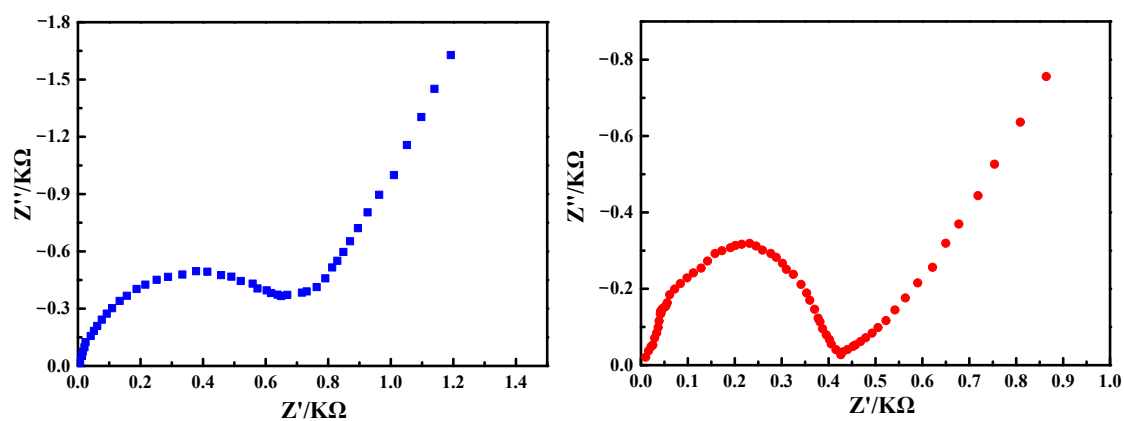


**Fig. S15** Nyquist plots of the pellet sample (a) compound **1** at 25 °C and 98% RH,  $S = 1.135 \text{ cm}^2$ ,  $L = 0.125 \text{ cm}$ . (b) compound **2** at 25 °C and 98% RH,  $S = 1.135 \text{ cm}^2$ ,  $L = 0.098 \text{ cm}$ .